The published version of the paper "M.P. Arrieta, E. Fortunati, F. Dominici, J. López, J.M. Kenny (2015). Bionanocomposite films based on plasticized PLA–PHB/cellulose nanocrystal blends, Carbohydrate Polymers, 121, 265-275" is available at: https://doi.org/10.1016/j.carbpol.2014.12.056

Bionanocomposite films based on plasticized PLA–PHB/cellulose nanocrystal blends

M.P. Arrieta[a], E. Fortunati[b],* F. Dominici[b], J. López[a], J.M. Kenny[b,ca]

[a]*Instituto de Tecnología de Materiales, Universitat Politècnica de Valencia, 03801 Alcoy-Alicante, Spain*
[b]*Materials Engineering Centre, UdR INSTM, NIPLAB, University of Perugia, 05100 Terni, Italy*
[c]*Institute of Polymer Science and Technology, CSIC, Juan de la Cierva 3, Madrid 28006, Spain*

Abstract

Optically transparent plasticized poly(lactic acid) (PLA) based bionanocomposite films intended for food packaging were prepared by melt blending. Materials were plasticized with 15 wt% of acetyl(tributylcitrate) (ATBC) to improve the material processability and to obtain flexibile films. Poly(hydroxybutyrate)(PHB) was used to increase PLA crystallinity. The thermal stability of the PLA–PHB blends was improved by the addition of 5 wt% of cellulose nanocrystals (CNC) or modified cellulose nanocrystals (CNCs) synthesized from microcrystalline cellulose. The combination of ATBC and cellulose nanocrystals, mainly the better dispersed CNCs, improved the interaction between PLA and PHB. Thus, an improvement on the oxygen barrier and stretchability was achieved in PLA–PHB–CNCs–ATBC which also displayed somewhat UV light blocking effect. All bionanocomposite films presented appropriate disintegration in compost suggesting their possible applications as biodegradable packaging materials.

1. Introduction

The use of bio-based and biodegradable polymers for food pack-aging applications is currently increasing in order to reduce the consumption of non-renewable resources and prevent the accumulation of plastics waste, respectively. Simultaneously, the food packaging industry demands the development of simple packaging formulations produced by easy, readily available and cost effective processing technologies such as melt blending approaches (Arrieta, Fortunati, et al., 2014b). At the same time, consumers demand high quality food with long shelf-life and also they desire see through the packaging to perceive the foodstuff aspect. Thus, food packaging are required to contain food products and protect them from the surroundings avoiding contamination, humidity and oxidations process as well as being enough transparent to allow seeing the food thought the packaging. Poly(lactic acid) (PLA) is the most used biopolymer as short term film for food packaging, due to its many advantages such as high transparency, availability in the market, ease of processing, economically competitive and environmentally benign characteristics

(Armentano et al., 2013; Auras, Harte, & Selke, 2004). In view of the fact that PLA also shows some poor

barrier properties, increasing PLA crystallinity become necessary for the intended use. Thus, melt blending PLA with another more crystalline biopolymer with similar melting temperature, such as poly(hydroxyalkanoates) (PHAs),has gain considerable attention for the food packaging sector. Among PHAs, poly(hydroxybutyrate) (PHB), produced by con-trolled bacterial fermentation, is the most common representative of PHA (Zhang & Thomas, 2011) and also widely studied for food packaging applications (Bucci, Tavares, & Sell, 2007).The miscibility between PLA and PHB is dependent on the processing temperature, the proportion and the molecular weight of the second component. PLA shows partial miscibility with low molar mass PHB (Hu, Sato, Zhang, Noda, & Ozaki, 2008) while presents optimal miscibility in the melt state (Blümm & Owen,1995). It has been reported that some transesterification reactions among PLA and PHB chains take place when they are melt blended in 75:25 proportion (Zhang & Thomas, 2011; Zhang, Xiong,& Deng, 1996). As a result, melt blending PLA with 25 wt% of fully bio-based and biodegradable poly(hydroxybutyrate) have gained special interest in the development of films for food packaging sector. The addition of highly ordered stereochemical structure of PHB at this proportion, produces a reinforcing effect since it crystallizes as small spherulites that act as nucleating agents for PLA(Zhang & Thomas, 2011), increasing its crystallinity (Abdelwahabet al., 2012; Arrieta, Fortunati, et al., 2014a; Arrieta, Fortunati,et al., 2014b; Arrieta, López, Hernández, & Rayón, 2014; Arrieta,Samper, López, & Jiménez, 2014) and, thus, improving the film final barrier properties (Arrieta, Fortunati, et al., 2014b; Arrieta,López, Hernández, et al., 2014; Arrieta, Samper, et al., 2014). More-over, PLA–PHB (75:25) blends showed increased Young's modulus(Arrieta, Fortunati, et al., 2014b; Arrieta, López, Hernández, et al.,2014; Arrieta, Samper, et al., 2014) and somewhat higher UV block-ing than neat PLA (Arrieta, Fortunati, et al., 2014b). Conversely, PHBhas small processing window, showing the melting temperature, at about 170–180◦C, close to the degradation temperature, typically centered at 270◦C (Koller, Salerno, Dias, Reiterer, & Braunegg,2010). As a consequence, PLA–PHB blends show lower thermal stability with respect to neat PLA (Arrieta, López, Hernández, et al.,2014; Arrieta, Samper, et al., 2014).On the other hand, a new approach is growing up in the packaging sector focused on the development of bio-based nanocomposites (bionanocomposites) since the addition of nanofillers lead to an enhancement in the thermomechanical performance, of bio-based polymers (Armentano et al., 2013; Rhim,Park, & Ha, 2013). To guarantee the packaging green nature, the ideal nanoparticles should be bio-based and biodegradable. Cellulose derivatives are optimal reinforcing materials for bioplastics industry since they are bio-based, biodegradable, stiff, lightweight, non-abrasiveness to the processing equipment and highly abundant in the nature at low cost (Brinchi, Cotana, Fortunati, & Kenny,2013; Frone, Berlioz, Chailan, & Panaitescu, 2013; Rayón, Ferrandiz,Rico, López, & Arrieta, 2014). Hence, cellulose nanocrystals (CNC),extracted from several plant fiber crops, have proven to be promising filler for the production of PLA based bionanocomposite films intended for food packaging (Fortunati, Armentano, Zhou, Iannoni,et al., 2012; Fortunati, Armentano, Zhou, Puglia, et al., 2012;Fortunati et al., 2014; Fortunati, Peltzer, Armentano, Jiménez, &Kenny, 2013;

Fortunati, Peltzer, et al., 2012). The homogeneous dispersion of high polarity CNC into the hydrophobic polymers matrices, such as the case of PLA and PHB, could be favored modifying the nanocrystal surfaces by their hydroxyl group interaction with a surfactant, leading to CNC surface functionalization (CNCs)(Fortunati, Armentano, Zhou, Iannoni, et al., 2012). In previous works, the processing performance, compatibility and thermal stability of PLA–PHB (75:25) blend were improved by the addition of5 wt% of nanocellulose (CNC) and eventually modified by means a surfactant (CNCs) synthesized from microcrystalline cellulose(MCC) by acid hydrolysis (Arrieta, Fortunati, et al., 2014a). The strat-egy of modified CNCs allows to obtain ternary bionanocomposite films with improved properties for the food packaging field: fully biodegradable, increased tensile properties, optimal transparency with somewhat UV blocking effect, improved oxygen barrier and water resistance (Arrieta, Fortunati, et al., 2014b).Another PLA–PHB blends drawback for film manufacturing is the inherent brittleness of PLA and PHB (Arrieta, Samper, et al., 2014).Plasticization is often used to improve biopolymers processability and other properties required for food packaging applications. In this sense, the use of plasticizers has demonstrated to be an effective way to improve the processability of PLA–PHB blends, at the same time that increased the stretchability of the obtained films (Abdelwahab et al., 2012; Arrieta, Castro-López et al., 2014;Arrieta, López, Hernández, et al., 2014; Arrieta, Samper, et al.,2014) and sped up the polymer disintegration in compost co-ditions, in relation to their post-use (Arrieta, López, Hernández,et al., 2014; Arrieta, López, Rayón, & Jiménez, 2014). Acetyl tributyl citrate (ATBC), obtained from naturally occurring citric acid and accepted to be in contact with food products (European Food Safety Authority, 2012), at 15 wt% has shown effectiveness to increase PLA–PHB blend elongation at break better than other plasticizers such as poly(ethylene glycol) (PEG) (Arrieta, Samper, et al.,2014) and d-limonene (Arrieta, López, Hernández, et al., 2014).Although, the addition of plasticizers make easy PLA and PHB chain mobility increasing the material oxygen permeability, plasticized PLA–PHB blends with ATBC showed lower oxygen permeation than those PLA–PHB blends plasticized with other plasticizers such as PEG (Arrieta, Samper, et al., 2014) and d-limonene (Arrieta, López,Hernández, et al., 2014).The main objective of the present research is to develop high performance and multifunctional flexible bionanocomposite films based on PLA–PHB blends through melt blending technology with improved properties for biodegradable food packaging pro-poses. Since the use of preformed masterbatches is a useful and cost-effective technique for industrial applications, PLA–PHB masterbatches were prepared by melt extrusion. Subsequently, PLA and PLA–PHB masterbatch were reinforced with synthesized cellulose nanocrystals (CNC) or modified cellulose nanocrystals (CNCs) and further plasticized with ATBC through melt blending technology directly followed by a film forming process. The influence of the plasticizer addition on the processing of the innovative quaternary systems was reported. The structural, thermal and mechanical properties of the obtained films were evaluated. Moreover, since these materials are intended for the biodegradable food packaging sector, surface

wettability, oxygen barrier, UV-blocking effect and the transparency were studied as well as their disintegration under composting conditions at a laboratory-scale level.

2. Experimental

2.1. Materials

Poly(lactic acid) (PLA 2002D, Mn= 98,000 g mol−1,4 wt% d-isomer) was supplied by Nature Works (USA) and poly(hydroxybutyrate) (PHB) was acquired by NaturePlast (France). Microcrystalline cellulose (MCC, dimensions of10–15 1m) and acetyl tributyl citrate (ATBC, M = 402 g mol−1,98% purity) were purchased from Sigma–Aldrich.

2.2. Cellulose nanocrystal synthesis and modification

Cellulose nanocrystals (CNC) were synthesized from microcrystalline cellulose by a sulphuric acid hydrolysis (64 wt/wt%) at 45◦Cfor 30 min with continuous stirring following the recipe used byFortunati and colleagues (Fortunati, Armentano, Zhou, Iannoni,et al., 2012).An acid phosphate ester of ethoxylated nonylphenol (STEFACTM 8170, Stepan Company, Northfield) was used in 1/1 (wt/wt) to modify the surface of CNC (CNCs).A freeze-drying procedure was conducted to obtain CNC and CNCs powders. The yield reaction resulted in ca. 21 ± 5% and the obtained nanocrystals displayed dimensions ranging from 100 to300 nm in length and between 5 and 10 nm in width (Arrieta,Fortunati, et al., 2014a).

2.3. Bionanocomposite preparation

Bionanocomposites were manufactured by using a twin-screw microextruder (DSM explorer 5&15 CC Micro Compounder) at screw speed of 150 rpm and mixing time of 3 min. While PLA pellets and ATBC were previously dried overnight at 80◦C, PHB pellets and cellulose nanocrystals (CNC and CNCs) were dried at 40◦C for4 h. PLA and PLA–PHB (75:25) blends were plasticized with 15 wt% ofATBC according with previous work (Arrieta, Samper, et al., 2014).Plasticized PLA and PLA–PHB were reinforced with 5 wt% of CNC or CNCs (Arrieta, Fortunati, et al., 2014a; Fortunati, Armentano, Zhou,Iannoni, et al., 2012).PLA pellets, were put in the microextruder manually to reach a head force of 1200 N using a mixing temperature profile with a maximum temperature of 200◦C by means three-step temperature procedure of 180–190–200◦C and a screw speed of 150 rpm. After 2 min, nanocrystals (CNC or CNCs) and ATBC were added into the microextruder for 1 additional minute. In the case of PLA–PHB blends, a masterbatch was previously prepared following the same processing conditions as described in a previous work(temperature procedure of 180–190–200◦C at 150 rpm for 2 min)(Arrieta, Fortunati, et al., 2014a). Preformed PLA–PHB masterbatch granulated into pellets was melted in the microextruder for 1 min reaching a head force of 1200 N. ATBC and/or nanocrystals (CNC or CNCs) were subsequently added and mixed during 1 extra minute. The addition of nanoreinforcements produced an increment in the force of the system, from 1000 N to around

1200 N in the case o CNC and to around 1400 N for CNCs (Arrieta, Fortunati, et al., 2014a),meanwhile the force decreased to in the region of 800–1000 N with the addition of ATBC. Directly after the mixing process, a film forming process was conducted to obtain plasticized PLA and PLA–PHB based bio-nanocomposite films with a thickness ranged from 10 to 30 μm. Neat PLA and PLA–PHB blend films were also produced for comparison. The obtained binary, ternary and quaternary formulations are shown in Fig. 1 and the proportion of each component is summarized in Table 1.

2.4. Characterization techniques

2.4.1. UV–vis spectrometry

The absorption spectra in the 700–250 nm region of bio-nanocomposite films were investigated by a Perkin Elmer (Lambda35, USA) UV–vis spectrophotometer.

2.4.2. Transmission electron microscopy (TEM)

The incorporation of CNC and CNCs into polymer matrix was studied by TEM. The bionanocomposite films cross section were embedded in epoxy resin and cured during 3 days at room temper-ature. Resins, containing the plasticized bionanocomposite films, were cut with an ultra-microtome (Leica CM1950, SCSIE Universitat de València) and then stained with a uranyl-acetate solution (2 wt% for 5 min). TEM images were obtained by transmission electron microscopy (TEM, JEOL JEM-1010) operating at 100 kV.

2.4.3. Field emission scanning electron microscope (FESEM)

The microstructure of bionanocomposite film cross sections, previously frozen in liquid nitrogen, cryofractured and sputtered with a gold layer, were observed by FESEM (Supra 25-Zeiss).

2.4.4. X-ray diffraction

The crystalline phases of the bionanocomposites were examined by X-ray diffraction (XRD) equipment (BRUKER AXS D5005,SCSIE Universitat de València). Scanning was performed on square bionanocomposite film surfaces (15 mm × 15 mm) mounted in an appropriate sample holder. The patterns were obtained from a diffractometer using Cu K1radiation with a scanning step of 0.02◦between 2.5◦and 40◦in 21 with a collection time of 10 s per step, while the voltage was held at 40 kV.

2.4.5. Fourier transformed infrared spectroscopy (FTIR)

FTIR measurements of plasticized nanocomposite films were conducted at room temperature in transmission mode by a Jasco FTIR-615 spectrometer. Spectra were obtained in the4000–600 cm−1region.

2.4.6. Thermogravimetric analysis (TGA)

Thermogravimetric measurements were performed by a Seiko Exstar 6300 thermal analyzer. Isothermal tests were carried outat a 200◦C during 40 min under air conditions while dynamic measurements were run from 30 to 900◦C at 10◦min−1under nitrogen atmosphere.

2.4.7. Differential scanning calorimetry (DSC)

DSC experiments were carried out by a TA Instrument Q200calorimeter (New Castle, DE, USA). The heating and cooling rate for the scans was 2◦C min−1under nitrogen atmosphere with sample weight about 4 mg in hermetic aluminum pans. A first heating scan from −25 to 210◦C at a heating rate of 2◦C min−1, followed by a cooling process up to −25◦C and subsequent heating up to 210◦Cwere applied. The glass transition temperature (Tg) was taken at the mid-point of heat capacity changes. The melting temperature (Tm) and cold crystallization temperature (Tcc) were obtained from the first heating while the degree of crystallinity (X_c) was calculated through Eq.(1).

$$\chi_c = 100\% \times \left[\frac{\Delta H_m - \Delta H_{cc}}{\Delta H_m^c}\right] \times \frac{1}{W_{PLA}} \quad \textbf{(1)}$$

Where ΔHmis the melting enthalpy, ΔHcc is the cold crystallizationenthalpy, ΔHcm is the melting heat associated to pure crystalline PLA (93 J g−1) (Bucci et al., 2007) and W_{PLA} the weight fraction of PLA in the blend.

2.4.8. Tensile test

The mechanical behavior of different formulations was investigated by tensile test in a digital Lloyd instrument LR 30K.Rectangular probes (100 mm × 10 mm) at room temperature by following the UNE-EN ISO 527-3 standard with a crosshead speed of 5 mm min−1, a load cell of 500 N and an initial gauge length of 50 mm were investigated. Average Young's modulus (E), tensile strength (1B), elongation at break (εB%) and yield stress and strain(εY%, 1Y) were calculated from the resulting stress–strain curves as the average of five measurements of each bionanocomposite film.

2.4.9. Oxygen transmission rate (OTR)

The oxygen transmission rate (OTR) was measured by means a Systech Instruments 8500 oxygen permeation analyzer (Metrotec S.A., Spain) at room temperature and 2.5 atm. 14 cm diameter circle films were compressed between the upper and lower diffusion chamber. Pure oxygen (99.9% purity) was introduced into the upper half of the sample chamber while nitrogen was injected into the lower half. To prepare the appropriate samples for OTR measurements, masterbatch pellets were set in discs by using a DSM Xplore10 ml injection molding machine at 175, 180 and 190◦C with a pressure profile in three steps (6 bar for 4 min, 8 bar for 5 min and8 bar for 3 min). The obtained discs were then processed into films by

compression molding process at 180◦C in a hot press (Mini C3850, Caver, Inc., Wabash, IN, USA) with a pressure cycle of 3 MPa for 1 min, 5 MPa for 1 min, and 10 MPa for 2 min. Plasticized bio-nanocomposite films were then quenched to room temperature at atmospheric pressure. Their average thickness was between 180and 250 m.

2.4.10. Static contact angle measurements

Surface wettability of films was studied through static water contact angle measurements by using a standard goniometer(EasyDrop-FM140, KRÜSS GmbH, Hamburg, Germany) equipped with a camera and Drop Shape Analysis SW21; DSA1 software was used to test the water contact angle (1◦). The contact angle was determined at room temperature by randomly putting five drops of distilled water (~2 l) with a syringe onto the film surfaces and, after 30 s, the average values of ten measurements for each drop were used.

2.5. Disintegration under composting conditions

The disintegration in composting conditions of different formulations was tested according to the ISO 20200 standard (UNE ENISO 20200, 2006). All films (cut in 15 mm × 15 mm) were weighed and buried at 4–6 cm depth in perforated plastic boxes contain-ing a solid synthetic wet waste prepared with 10% of compost(Gesenu S.p.a., Perugia, Italy), 30% rabbit food, 10% starch, 5% sugar,1% urea, 4% corn oil and 40% sawdust and approximately 50 wt% of water content. Samples were then incubated at aerobic conditions at 58◦C. Films were recovered at 1, 2, 7, 10 and 14 days of disintegration, cleaned with distilled water, dried in an oven at37◦C during 24 h and reweighed. The time at which 50% of the film was disintegrated (t50) was estimated by correlating the obtained data with the Boltzmann equation (OriginPro 8.1. software) as follows:

$$m = \frac{(m_i - m_\infty)}{1 + e^{(1 - t_{50}/d_t)}} \qquad (2)$$

where mi and m∞ are the initial and final mass values measured respectively at the beginning of the exposition to compost and after the final asymptotes of the disintegrability test, and t50is the time at which materials disintegrability reaches the average value between mi and m∞, known as the half-maximal degradation, dt is a parameter that describes the shape of the curve between the upper and lower asymptotes (Arrieta, Parres, López, & Jiménez, 2013). The dis-integration degree at different days of incubation was calculated by normalizing the sample weight to the initial weight. Thus, mi is 0%and m∞ is 100%.

3. Results and discussions

3.1. Visual appearance and optical characterization

The processing technology used in the present work allowed obtaining thin films with thickness ranging between 10 and 30 m. Thus, all formulations resulted mostly transparent allowing seeing through the film, even those formulations with 25 wt% of commonly amber PHB (Fig. 1A). These results were confirmed by means of the determination of the optical properties by absorption measurements in the range of 540–560 nm of the visible region of the spectra (Auras et al., 2004). While neat PLA sample was the most transparent film, PLA–PHB showed the lowest light trans-mission (Fig. 1B). Cellulose nanocrystals, either pristine CNC or surfactant modified CNCs, and ATBC addition, slightly improved the transparency of PLA–PHB. No significant changes were observed on the light transmission along the visible region of the spectra(400–700 nm) suggesting that CNC and/or CNCs were homogeneous dispersed in PLA and PLA–PHB matrix (Arrieta, Fortunati,et al., 2014a; Fortunati, Armentano, Zhou, Iannoni, et al., 2012).Regarding the UV spectra region (250–400 nm), PHB and cellulose nanocrystals, particularly CNCs, show a blocking effect on the ultraviolet C region (280–100 nm), usually produced by artificial light sources (Auras et al., 2004).

3.2. Morphological and structural characterizations

The effective incorporation of CNC and CNCs into polymer matrices was verified by TEM investigation. Fig. 1C shows individual well defined rod-like nanocrystals, both pristine CNC(inset Fig. 1C-a and upper c) and surfactant modified CNCs (inset Fig. 1C-b and d), with dimensions ranging from 100 to 300 nm identified in plasticized PLA and PLA–PHB matrices. As a result of the low contrast between PLA, PHB and cellulose structures, was very difficult to study the CNC and CNCs distribution by TEM (Bondeson, Mathew, & Oksman, 2006; Fortunati, Armentano, Zhou,Iannoni, et al., 2012). Nevertheless, in the pristine CNC based bio-nanocomposites, it was possible to detect some CNC agglomerates into flakes (black arrow in Fig. 1C-a and lower inset c) consisting in tightly packed cellulose nanocrystals; the agglomeration phenomena are due to strong hydrogen bonds established between the nanocrystals (Fortunati, Armentano, Zhou, Iannoni, et al.,2012), that seems not appear in surfactant modified based films. Higher level of dispersion is expected for CNCs in PLA (Fortunati,Armentano, Zhou, Puglia, et al., 2012; Fortunati, Peltzer, et al.,2012) and PLA–PHB (Arrieta, Fortunati, et al., 2014a) matrices. Thenanocrystal surface modification allows the polymers chain pen-etration between the cellulose structures. Furthermore, the ATBC addition promotes an enhancement of the PLA and PHB chains mobility (Arrieta, Samper, et al., 2014), which should contribute to increase the nanocrystal dispersion within the polymer matrices. Fig. 2A shows the FESEM micrographs of the cross-fractured sections of plasticized PLA and PLA–PHB bionanocomposite films. As expected PLA (Fig. 2A-a) exhibits a regular and smooth surface of amorphous polymers, whereas PLA–PHB (Fig. 2A-b) presents amore roughness surface containing some voids of different sizes. Plasticized PLA films show a clear more plastic deformation and no apparent phase separation as a result of the homogeneous

dispersion of ATBC in PLA (Fig. 2A-c), PLA–CNC–ATBC (Fig. 2A-d)and PLA–CNCs–ATBC (Fig. 2A-e) matrices confirming the efficiency of ATBC as plasticizer for PLA based materials (Courgneau,Domenek, Guinault, Averous, & Ducruet, 2011). The fracture surface of PLA–PHB–ATBC (Fig. 2A-f) exhibits a rougher surface andalso shows some voids. These voids disappeared with the introduction of CNC or CNCs into the PLA–PHB–CNC–ATBC (Fig. 2A-g) andPLA–PHB–CNCs–ATBC (Fig. 2A-h) systems, highlighting the positive effect of cellulose nanostructures presence in the PLA–PHB matrices. In a previous work the appearance of cellulose nanocrystals in flakes with poor interfacial adhesion was observed in binary PLA–CNC (Fortunati, Armentano, Zhou, Iannoni, et al., 2012) andternary PLA–PHB–CNC systems (Arrieta, Fortunati, et al., 2014a), meanwhile these flakes were less formed in surfactant modified based nanocomposites (Arrieta, Fortunati, et al., 2014a; Fortunati,Armentano, Zhou, Iannoni, et al., 2012; Fortunati, Peltzer, et al.,2012).

In this work, the appearance of holes as well as cellulose nanocrystals in flakes is not observed in PLA–PHB–CNC–ATBC(Fig. 2A-g) and PLA–PHB–CNCs–ATBC (Fig. 2A-h) most likely due tothe ATBC presence that facilitates the processing of PLA and PHB by reducing the force and the viscosity in the system and, thus, it could favor the dispersion of CNC and CNCs within the polymer matrices during processing. The crystalline structure of the developed films was investigated by X-ray diffraction (Fig. 2B). The X-ray pattern of all PLA based films displays a peak at 21 = 16.5◦characteristic of the reflection of PLA crystals. The expected diffraction peaks of cellulose I (21 = 14.8◦,16.5◦, 22.5◦and 34.5◦) were not observed in nanocellulose based films, probably attributable to the low cellulose nanocrystal con-tent (5 wt%) used and, thus, these signals in the blend might be masked by the PLA crystalline diffraction (Bitinis et al., 2013).PLA–PHB and PLA–PHB–ATBC displayed the typical reflection peaks of PHB at 21 = 13◦and 21 = 17◦, in addition to the three weak peaks at higher 21 (19.8◦, 22.2◦and 25◦) (Abdelwahab et al., 2012). In the case of PLA–PHB–ATBC the peaks at 21 = 13◦and 21 = 17◦ showed increased intensity. The diffraction patterns of the qua-ternary systems PLA–PHB–CNC–ATBC and PLA–PHB–CNCs–ATBC did not reveal signals of crystallinity. However, this indicates that the crystal structured observed in PLA–PHB–ATBC was distorted due the positive effect of plasticizer on the dispersion of cellulose nanocrystal in the polymer matrices. The final properties of nanocomposites depend not only on the properties of each constituent but also on the interactions among all of them, particularly those chemical aspects related to the polymer–nanofiller interactions (Navarro-Baena, Kenny, &Peponi, 2014). The FTIR analysis (Fig. 2C) showed that the typical stretching band of the carbonyl group centered at 1750 cm−1pre-sented a shoulder at 1720 cm−1in PLA–PHB and PLA–PHB–ATBC blend due to the crystalline carbonyl stretching of PHB (Zhang& Thomas, 2011). These bands became one broader band in PLA–PHB/cellulose nanocrystal based films (PLA–PHB–CNC–ATBC and PLA–PHB–CNCs–ATBC) most likely due to hydrogen bond inter-action between the carbonyl groups of PLA, PHB and ATBC andhydroxyl groups of cellulose, as is proposed in Fig. 3, that are favoring the interaction among all the blend components. The hydroxyl groups of cellulose tend to interact by hydrogen bond interaction and these interactions have been previously suggested in PLA–cellulose nanocrystals based nanocomposites

(Martínez-Sanz, Lopez-Rubio, & Lagaron, 2014) and also between the hydroxyl groups of CNC and the carbonyl groups of PHB (Patrício et al., 2013).

3.3. Thermal properties of bionanocomposite films

Cellulose nanocrystals were incorporated with the main objective to enhance the interfacial adhesion between PLA and PHB and, thus, improve the thermal stability of the materials. As well, they were added to increase the temperature region where PLA–PHB blend can be processed without risk of thermal degradation(Arrieta, Fortunati, et al., 2014a). In this work, thermogravimetric analysis (TGA) was conducted to study the influence of the addition of a plasticizer on the thermal degradation properties of PLA(Fig. 4A) and PLA–PHB (Fig. 4B) formulations and the main thermal parameters obtained from TGA and DTG curves are summarized in Table 2.PLA degraded in a single step process, while PLA–ATBC, PLA–PHB and PLA–PHB–ATBC blends degraded in a two-step process in accordance with previous reported works (Arrieta, Castro-López et al., 2014; Arrieta, Samper, et al., 2014). The plasticizer presence decreased the onset degradation temperature (T0) of PLA (Table 2),in good agreement with other PLA-plasticized materials (Burgos,Martino, & Jiménez, 2013; Martino, Jiménez, & Ruseckaite, 2009;Scatto et al., 2013) and PHB-plasticized materials (Erceg, Kovacic,& Klaric, 2005).From the DTG curve of Fig. 4A could be observed that PLA–ATBC presents a degradation peak prior to the PLA degradation signal that has been related with plasticizer vaporization (Arrieta,Samper, et al., 2014). TGA curves of reinforced plasticized PLA(PLA–CNC–ATBC and PLA–CNCs–ATBC, Fig. 4A) and reinforced plasticized PLA–PHB (PLA–PHB–CNC–ATBC and PLA–PHB–CNCs–ATBC,Fig. 4B) show that reinforced plasticized systems follow a one-step thermal degradation process. These results confirm the positive effect of CNC and CNCs on the interaction between PLA, ATBC, and/or PHB, verifying the occurrence of polymer–nanofiller inter-actions. Nevertheless, from DTG curves is possible to see a small shoulder within the degradation temperature range of ATBC which is more evident in the case of plasticized PLA reinforced systems(Fig. 4A) than in plasticized PLA–PHB reinforced system (Fig. 4B),where the degradation of ATBC is partially overlapped to the main peak of the polymer degradation. On the other hand, the addition of CNC shifted the onset degradation process (T0) of the bionanocomposites to higher temperatures leading to an improvement in the thermal stability of PLA–CNC–ATBC and PLA–PHB–CNC–ATBC. Meanwhile, the addition of modified CNCs shifted the T0of plasticized PLA towardlower temperatures (around 18◦C) and also slightly decreased theT0 of plasticized PLA–PHB blends (about 4◦C). It should be noticed that no degradation takes place in the temperature region from room temperature to 200◦C, where the bionanocomposites were processed and/or are intended to be used. Fig. 4C and D shows the DSC curves during the first heating scan of plasticized PLA films and plasticized PLA–PHB films, respectively while the DSC properties are summarized in Table 2. As expected, a decrease in glass transition temperature was observed in the plasticized PLA samples. This reduction was particularly noticeable in PLA–CNCs–ATBC. The addition of ATBC also reduced the glass transition temperature of PLA–PHB blend.

However, an increase in Tg values was observed for PLA–PHB–CNC–ATBC and PLA–PHB–CNCs–ATBC, with respect to the unfilled PLA–PHB–ATBC, in accordance with previous results (Arrieta, Fortunati, et al.,2014a).Regarding the cold crystallization temperature, while in plasticized PLA based samples it decreased with respect to the neat PLA, Tcc values increased in plasticized PLA–PHB based materials with respect to PLA–PHB blend. In a previous work, it was also observed that cellulose nanocrystal presence produced a higher cold crystallization temperature values for PLA–PHB–CNC (70.9◦C) and PLA–PHB–CNCs (72.1◦C) than PLA–PHB blend (Arrieta, Fortunati,et al., 2014a). In the present work, the combination of cellulose nanocrystals with the plasticizer in the PLA–PHB blends produced higher cold crystallization temperature values and higher crystallinity degrees. The synergic effect on the crystallization of PLA produced by a potential nucleating agent and a plasticizer, has been previously observed by Courgneau, Ducruet, Avérous, Grenet,and Domenek (2013) in PLA reinforced with talc and plasticized with poly(ethylene glycol) (PEG) and/or ATBC (Courgneau, Ducruet,Avérous, Grenet, & Domenek, 2013). The higher crystallinity degree was found for the modified CNCs based nanocomposites as a consequence of the better dispersion of these nanocrystals in plasticized PLA and PLA–PHB matrices that promotes a higher nucleation effect (Arrieta, Fortunati, et al., 2014a; Fortunati, Armentano, Zhou,Iannoni, et al., 2012).ATBC slightly reduced the melting temperature of PLA in agreement with previous results (Arrieta, Samper, et al., 2014).PLA–PHB and PLA–PHB–ATBC showed a double melting behavior due to the melting of PLA at around 149◦C and the melting of PHB at about 171◦C. Although, a double melting behavior occurs it is possible to note that ATBC is lowering the Tm value of PLA and PHB in PLA–PHB–ATBC sample confirming its efficiency as plasticizer for both, PLA (Courgneau, Ducruet, Avérous,Grenet, & Domenek, 2013; Scatto et al., 2013) and PHB (Erceget al., 2005; Wang et al., 2008). Meanwhile, the addition of cellulose nanocrystals leaded to mainly one peak centered at 147◦Cas a result of nanocellulose enhanced the interaction between PLA and PHB improving their compatibility. However, a small peak was shown in PLA–PHB–ATBC–CNC at approximately 165◦Cthat had been associated with the as-formed PHB crystals during blending process (Zhang & Thomas, 2011). Whereas, the better dispersed CNCs interact better with PLA, PHB and ATBC showing only one melting peak in PLA–PHB–ATBC–CNCs. This result shows that PLA–PHB–CNCs–ATBC could be melt processed in the region from 155◦C to 190◦C, considerable improving the usually narrow processing window of PHB whose shows somewhat thermal degradation such as random scission of long PHB chains at higher temperatures than 190◦C (Erceg et al.,2005).

3.4. Mechanical characterization

The mechanical behavior of plasticized different formulations was evaluated and tensile test results are reported in Table 3. The addition of ATBC mostly reduced the tensile strength (σB), Young's modulus (E) and yield strain (εY) of PLA and PLA–PHB films, as the same time as it increases the elongation at break (εB%) withrespect of the un-plasticized films previously reported (Arrieta,Fortunati, et al., 2014a).All

bionanocomposites showed comparable values of yield strain and tensile strength. Nevertheless, the addition of CNC or CNCs showed different influences on the mechanical behavior of the plasticized bionanocomposites. The incorporation of CNC to plasticized PLA and PLA–PHB materials did not show significant reductions on the Young's modulus, whilst the incorporation of CNCs produced considerable lower E values. As well, surfactant modified cellulose nanocrystal based systems presented significant higher values of elongation at break with respect of their pristine CNC based films. In this sense, the highest elongation at break was obtained in quaternary bionanocomposite with modified CNCs (PLA–PHB–CNCs–ATBC) as a consequence of the positive effect of the modification of cellulose nanocrystals that produce better interaction between PLA and PHB allowing the higher elongation at break (Arrieta, Fortunati, et al.,2014a) which could be further increased by plasticization with ATBC which increased the polymers chains mobility reaching approximately to 150% and, accordingly, PLA–PHB–CNCs–ATBC showed the lowest Young's modulus. The increase in the elongation at break and the reduction in the Young's modulus produced by ATBC have been previously observed in PLA–ATBC (Courgneauet al., 2011) and also in PHB–ATBC based materials (Wanget al., 2008). Films for food packaging are required for high flexibility at room temperature and the obtained value of elongation at break of PLA–PHB–CNCs–ATBC are comparable to those of commercial plasticized PVC stretching films (Fenollar et al.,2013).

3.5. Wettability and oxygen permeability

Since materials food packaging are required to protect foodstuff from humidity and oxidation processes, the hydrophilic/hydrophobic character of films was evaluated by water contact angle measurements and their oxygen barrie rproperties were studied by the determination of the oxygen transmission rate through the films. The addition of either pristine CNC or surfactant modified CNCs, and ATBC increased the surface wettabillity of PLA and PLA–PHB films (Table 3). Thus, both quaternary bionanocomposites(PLA–PHB–CNC–ATBC and PLA–PHB–CNCs–ATBC) and the ternary bionanocomposite with pristine CNC (PLA–CNC–ATBC) showed the most hydrophilic surfaces. However, ternary PLA–CNCs–ATBC did not show significant differences with PLA and PLA–ATBC film probably because of the better dispersed CNCs in PLA matrix exposed lower OH-groups on the film surface. Plasticized bionanocomposites showed lower water contact angle values with respect to their unplasticized counterparts previously reported (Arrieta, Fortunati,et al., 2014a), may be due of the plasticizing effect influence the diffusion process as a consequence of the increased polymer chain mobility (Fortunati et al., 2014).PLA presents low oxygen barrier properties for food packaging applications which further decrease owing to the incorporation of plasticizers (Arrieta, López, Ferrándiz, & Peltzer, 2013; Burgoset al., 2013; Martino et al., 2009). The combination of PHB, modified cellulose nanocrystals (CNCs) and ATBC produced a OTR value of 23.3 cm3mm m−2day−1 for PLA–PHB–CNCs–ATBC qua-ternary bionanocomposite film, which means a reduction around24% in PLA OTR.e value (30.5 cm3mm m−2day−1) (Fortunati et al.,2013). As expected, the addition of ATBC in PLA–PHB–

CNCs–ATBC increased around 80% the oxygen permeation with respect to theun-plasticized PLA–PHB–CNCs (13 cm3mm m−2day−1) (Arrieta,Fortunati, et al., 2014b). The improve of PLA oxygen barrier proper-ties due to cellulose nanocrystals introduction, particularly surface modified CNCs (Fortunati, Peltzer, et al., 2012), as well as, due to it blend with the more crystalline PHB (Arrieta, López, Hernández,et al., 2014; Arrieta, Samper, et al., 2014) have been previously reported. In this work, the combination of PHB and CNCs improved the oxygen barrier properties of PLA, even with the addition of a plasticizer to the system highlighting the positive interaction between all the blend components. It should be highlighted that the OTR.e values for these blends are clearly lower than that of commercial low density polyethylene (LDPE), 160 cm3mm m−2day−1(Burgos et al., 2013).

3.6. Disintegration in composting conditions

The visual appearance of recovered films at different time of disintegration in composting conditions and the mass loss induced by the incubation times, are shown in Fig. 5. The films disintegrability was evaluated in terms of mass loss as a function of incubation time by using the Boltzmann equation, as shown in Fig. 5B, to calculate the half-maximal degradation (t50) (Table 3).Fig. 5A shows that films became smaller in one day in compost, in good accordance with previous work (Arrieta, Fortunati, et al.,2014b; Fortunati et al., 2014) with the exception of PLA–PHB and PLA–PHB–ATBC blends that started the film size reduction on the econd day in compost. PLA based films reach the goal of disintegrability test (90% of disintegration according to ISO 20200) in about 7 and 8 days, whereas PLA–PHB based films needed more than 12 days. PHB delayed the PLA disintegration rate since it acts as a nucleating agent increasing the crystallinity of PLA (Arrieta,Fortunati, et al., 2014b; Arrieta, López, Hernández, et al., 2014;Arrieta, López, Rayón, et al., 2014). Otherwise, a clear increase of the disintegration phenomenon was observed in PLA and PLA–PHBfilms due to the addition of both, ATBC (Arrieta, López, Rayón,et al., 2014) and cellulose nanocrystals (Arrieta, Fortunati, et al.,2014b). Thus, the half-maximal degradation decreased with respect of PLA or PLA–PHB. This reduction followed similar diminishing tendency to the surface water contact angle values (Table 3) since the polymer disintegration starts by a hydrolysis process. How-ever, PLA–PHB–CNCs–ATBC showed the most hydrophilic surface and discordantly the lower rate of disintegration. The wettability is strongly dependent on the surface chemical and topographical properties, but the water diffusion thought the polymer matrix is also highly affected by the crystallinity of the system (Fortunatiet al., 2014). PLA–PHB–CNCs–ATBC showed the highest crystallinity caused by the synergic effect of PHB, CNCs and ATBC on the crystallization of PLA (already commented in DSC results) and the crystalline regions are further resistant to hydrolysis and degradation processes. As expected, the ATBC presence increase the rate of disintegration of PLA based bionanocomposite films with respect of their un-plasticized counterparts previously reported (Arrieta,Fortunati, et al., 2014b). However, different behavior was observed for PLA–PHB based bionanocomposites where the presence of ATBC delayed the rate of disintegration. Thus, quaternary

bionanocomposites showed higher half-maximal degradation values (t50ofPLA–PHB–CNC–ATBC = 7.24 and t50PLA–PHB–CNCs–ATBC = 10.51)than the ternary un-plasticized corresponding films (t50PLA–PHB–CNC = 7.06 and t50PLA–PHB–CNCs = 9.93) (Arrieta,Fortunati, et al., 2014b). This unexpected slower disintegration rate of quaternary bionanocomposite films could be explained with the positive interaction of PLA, PHB with better dispersed CNC or CNCs as a result of the plasticizer presence (as suggested in Fig. 3), which slightly protect the polymer from the water and microorganisms attack.

4. Conclusions

Plasticized multifunctional bionanocomposite films based on PLA–ATBC and PLA–PHB–ATBC reinforced with synthesized CNC or surfactant modified CNCs were successfully developed and deeply characterized. A masterbatch of PLA–PHB was prepared to make easier the polymers processability and to increase the dispersion of cellulose nanocrystals. ATBC presence improved the polymers processability and consequently improved the dispersion of CNC and/or CNCs within the polymer matrices during processing and allowed the obtainment of homogeneous and flexible materials. PHB acted as nucleating agent increasing the PLA crystallinity required to enhance its barrier properties. The thermogravimetric analysis showed that while plasticized PLA–PHB sample degraded in two step process, the reinforced CNC or CNCs materials degraded in one step as a consequence of the better interaction between all components in the nanocomposites. Likewise, PLA–PHB and PLA–PHB–ATBC showed a double melting behavior whereas the quaternary nanocomposites, particularly PLA–PHB–CNCs–ATBC, not only showed one melting peak but also showed a reduction onthe melting of PHB leading to an improvement of the usually small processing window of the PHB. All bionanocomposite films resulted optically transparent due to their processing in thin films, even with PHB presence. The synergic effect of ATBC and the better dispersed modified CNCs, increased the elongation at break, enhanced the crystallization effect and improved the oxygen barrier properties of PLA–PHB blends. The disintegrability test confirmed the biodegradable character of all film formulations. Moreover, the plasticizer and CNC or CNCs are able to speed up the disintegration process of the produced bionanocomposites. These results suggest that multifunctional plasticized PLA–PHB blends reinforced with modified CNCs are promising materials as flexible films for food packaging.

Acknowledgments

Authors wish to acknowledge Spanish Ministry of Science and Innovation (MAT2011-28468-C02-01 and 02), Prof. A. Jimenez and Dr. Nuria Burgos (University of Alicante, Spain) for their assistancein OTR measurements and Gesenu S.p.a. for compost supply. M.P. Arrieta wishes to thank Generalitat Valenciana for Santiago Grisolía Fellowship (2011/007) and Universitat Politècnica de València for the Development Support Programme PAID-00-12 (SP20120120).

References

Abdelwahab, M. A., Flynn, A., Chiou, B. S., Imam, S., Orts, W., & Chiellini, E.(2012). Thermal, mechanical and morphological characterization of plasticized PLA–PHB blends. Polymer Degradation and Stability, 97(9), 1822–1828.

Armentano, I., Bitinis, N., Fortunati, E., Mattioli, S., Rescignano, N., Verdejo, R., et al.(2013). Multifunctional nanostructured PLA materials for packaging and tissueengineering. Progress in Polymer Science, 38(10–11), 1720–1747.

Arrieta, M. P., Castro-López, M. D. M., Rayón, E., Barral-Losada, L. F., López-Vilari˜no, J.M., López, J., et al. (2014). Plasticized poly(lactic acid)–poly(hydroxybutyrate)(PLA–PHB) blends incorporated with catechin intended for active food-packaging applications. Journal of Agricultural and Food Chemistry, 62(41),10170–10180.

Arrieta, M. P., Fortunati, E., Dominici, F., Rayón, E., López, J., & Kenny, J. M. (2014a).Multifunctional PLA–PHB/cellulose nanocrystal films: Processing, structural andthermal properties. Carbohydrate Polymers, 107, 16–24.

Arrieta, M. P., Fortunati, E., Dominici, F., Rayón, E., López, J., & Kenny, J. M. (2014b).PLA–PHB/cellulose based films: Mechanical, barrier and disintegration proper-ties. Polymer Degradation and Stability, 107, 139–149.

Arrieta, M. P., López, J., Ferrándiz, S., & Peltzer, M. A. (2013). Characterization ofPLA–limonene blends for food packaging applications. Polymer Testing, 32(4),760–768.

Arrieta, M. P., López, J., Hernández, A., & Rayón, E. (2014). TernaryPLA–PHB–limonene blends intended for biodegradable food packagingapplications. European Polymer Journal, 50(0), 255–270.

Arrieta, M. P., López, J., Rayón, E., & Jiménez, A. (2014). Disintegrability under com-posting conditions of plasticized PLA–PHB blends. Polymer Degradation andStability, 108, 307–318.

Arrieta, M. P., Parres, F., López, J., & Jiménez, A. (2013). Development of a novelpyrolysis-gas chromatography/mass spectrometry method for the analysis ofpoly(lactic acid) thermal degradation products. Journal of Analytical and AppliedPyrolysis, 101, 150–155.

Arrieta, M. P., Samper, M. D., López, J., & Jiménez, A. (2014). Combined effect ofpoly(hydroxybutyrate) and plasticizers on polylactic acid properties for filmintended for food packaging. Journal of Polymers and the Environment, 22,460–470.

Auras, R., Harte, B., & Selke, S. (2004). An overview of polylactides as packagingmaterials. Macromolecular Bioscience, 4(9), 835–864.

Bitinis, N., Verdejo, R., Bras, J., Fortunati, E., Kenny, J. M., Torre, L., et al. (2013).Poly(lactic acid)/natural rubber/cellulose nanocrystal bionanocomposites. PartI. Processing and morphology. Carbohydrate Polymers, 96(2), 611–620.

Blümm, E., & Owen, A. J. (1995). Miscibility, crystallization and melting of poly(3-hydroxybutyrate)/poly(l-lactide) blends. Polymer, 36(21), 4077–4081.

Bondeson, D., Mathew, A., & Oksman, K. (2006). Optimization of the isolation ofnanocrystals from microcrystalline cellulose by acid hydrolysis. Cellulose, 13(2),171–180.

Brinchi, L., Cotana, F., Fortunati, E., & Kenny, J. M. (2013). Production of nanocrys-talline cellulose from lignocellulosic biomass: Technology and applications.Carbohydrate Polymers, 94(1), 154–169.

Bucci, D. Z., Tavares, L. B. B., & Sell, I. (2007). Biodegradation and physical evaluationof PHB packaging. Polymer Testing, 26(7), 908–915.

Burgos, N., Martino, V. P., & Jiménez, A. (2013). Characterization and ageing study ofpoly(lactic acid) films plasticized with oligomeric lactic acid. Polymer Degrada-tion and Stability, 98(2), 651–658.

Courgneau, C., Domenek, S., Guinault, A., Averous, L., & Ducruet, V. (2011). Analysisof the structure–properties relationships of different multiphase systems basedon plasticized poly(lactic acid). Journal of Polymers and the Environment, 19(2),362–371.

Courgneau, C., Ducruet, V., Avérous, L., Grenet, J., & Domenek, S. (2013). Non-isothermal crystallization kinetics of poly(lactide) – Effect of plasticizers andnucleating agent. Polymer Engineering and Science, 53(5), 1085–1098.

Erceg, M., Kovaˇci´c, T., & Klari´c, I. (2005). Thermal degradation of poly(3-hydroxybutyrate) plasticized with acetyl tributyl citrate. Polymer Degradationand Stability, 90(2 SPEC. ISS.), 313–318.

European Food Safety Authority. (2012). Scientific opinion on flavouring groupevaluation 10, revision 3 (FGE.10Rev3): Aliphatic primary and secondary sat-urated and unsaturated alcohols, aldehydes, acetals, carboxylic acids and esterscontaining an additional oxygenated functional group and lactones from chemical groups 9, 13 and 30. EFSA Journal, 10(3), 2563.

Fenollar, O., Garcia-Sanoguera, D., Sanchez-Nacher, L., Boronat, T., López, J., & Balart,R. (2013). Mechanical and thermal properties of polyvinyl chloride plasticizedwith natural fatty acid esters. Polymer – Plastics Technology and Engineering,52(8), 761–767.

Fortunati, E., Armentano, I., Zhou, Q., Iannoni, A., Saino, E., Visai, L., et al. (2012). Mul-tifunctional bionanocomposite films of poly(lactic acid), cellulose nanocrystalsand silver nanoparticles. Carbohydrate Polymers, 87(2), 1596–1605.

Fortunati, E., Armentano, I., Zhou, Q., Puglia, D., Terenzi, A., Berglund, L. A., et al.(2012). Microstructure and nonisothermal cold crystallization of PLA com-posites based on silver nanoparticles and nanocrystalline cellulose. PolymerDegradation and Stability, 97(10), 2027–2036.

Fortunati, E., Luzi, F., Puglia, D., Dominici, F., Santulli, C., Kenny, J. M., et al. (2014).Investigation of thermo-mechanical, chemical and degradative properties ofPLA–limonene films reinforced with cellulose nanocrystals extracted fromPhormium tenax leaves. European Polymer Journal, 56(1), 77–91.

Fortunati, E., Peltzer, M., Armentano, I., Jiménez, A., & Kenny, J. M. (2013). Com-bined effects of cellulose nanocrystals and silver nanoparticles on the barrier andmigration properties of PLA nano-biocomposites. Journal of Food Engineering,118(1), 117–124.

Fortunati, E., Peltzer, M., Armentano, I., Torre, L., Jiménez, A., & Kenny, J. M.(2012). Effects of modified cellulose nanocrystals on the barrier and migra-tion properties of PLA nano-biocomposites. Carbohydrate Polymers, 90(2),948–956.

Frone, A. N., Berlioz, S., Chailan, J.-F., & Panaitescu, D. M. (2013). Morphology andthermal properties of PLA–cellulose nanofibers composites. Carbohydrate Poly-mers, 91(1), 377–384.

Hu, Y., Sato, H., Zhang, J., Noda, I., & Ozaki, Y. (2008). Crystallization behaviorof poly(l-lactic acid) affected by the addition of a small amount of poly(3-hydroxybutyrate). Polymer, 49(19), 4204–4210.

Koller, M., Salerno, A., Dias, M., Reiterer, A., & Braunegg, G. (2010). Modern biotech-nological polymer synthesis: A review. Food Technology and Biotechnology, 48(3),255–269

Martínez-Sanz, M., Lopez-Rubio, A., & Lagaron, J. M. (2014). Dispersing bacterialcellulose nanowhiskers in polylactides via electrohydrodynamic processing.Journal of Polymers and the Environment, 22(1), 27–40.

Martino, V. P., Jiménez, A., & Ruseckaite, R. A. (2009). Processing and characterizationof poly(lactic acid) films plasticized with commercial adipates. Journal of AppliedPolymer Science, 112(4), 2010–2018.

Navarro-Baena, I., Kenny, J. M., & Peponi, L. (2014). Thermally-activated shape mem-ory behaviour of bionanocomposites reinforced with cellulose nanocrystals.Cellulose, 21(6), 4231–4246.

Patrício, P. S. D. O., Pereira, F. V., Dos Santos, M. C., De Souza, P. P., Roa, J. P. B., & Orefice,R. L. (2013). Increasing the elongation at break of polyhydroxybutyrate biopoly-mer: Effect of cellulose nanowhiskers on mechanical and thermal properties.Journal of Applied Polymer Science, 127(5), 3613–3621.

Rayón, E., Ferrandiz, S., Rico, M. I., López, J., & Arrieta, M. P. (2014). Microstructure,mechanical and thermogravimetric characterization of cellulosic by-productsobtained from the biomass seeds. International Journal of Food Properties,http://dx.doi.org/10.1080/10942912.2014.884578

Rhim, J.-W., Park, H.-M., & Ha, C.-S. (2013). Bio-nanocomposites for food packagingapplications. Progress in Polymer Science, 38(10–11), 1629–1652.

Scatto, M., Salmini, E., Castiello, S., Coltelli, M. B., Conzatti, L., Stagnaro, P., et al. (2013).Plasticized and nanofilled poly(lactic acid)-based cast films: Effect of plasticizerand organoclay on processability and final properties. Journal of Applied PolymerScience, 127(6), 4947–4956.

UNE EN ISO 20200. (2006). Determination of the degree of disintegration of plasticmaterials under simulated composting conditions in a laboratory-scale test.

Wang, L., Zhu, W., Wang, X., Chen, X., Chen, G.-Q., & Xu, K. (2008). Processability mod-ifications of poly(3-hydroxybutyrate) by plasticizing, blending, and stabilizing.Journal of Applied Polymer Science, 107(1), 166–173.

Zhang, L., Xiong, C., & Deng, X. (1996). Miscibility, crystallization and morphology ofpoly(_-hydroxybutyrate)/poly(d,l-lactide) blends. Polymer, 37(2), 235–241.Zhang, M., & Thomas, N. L. (2011). Blending polylactic acid with polyhydroxy-butyrate: The effect on thermal, mechanical, and biodegradation properties.Advances in Polymer Technology, 30(2), 67–79.

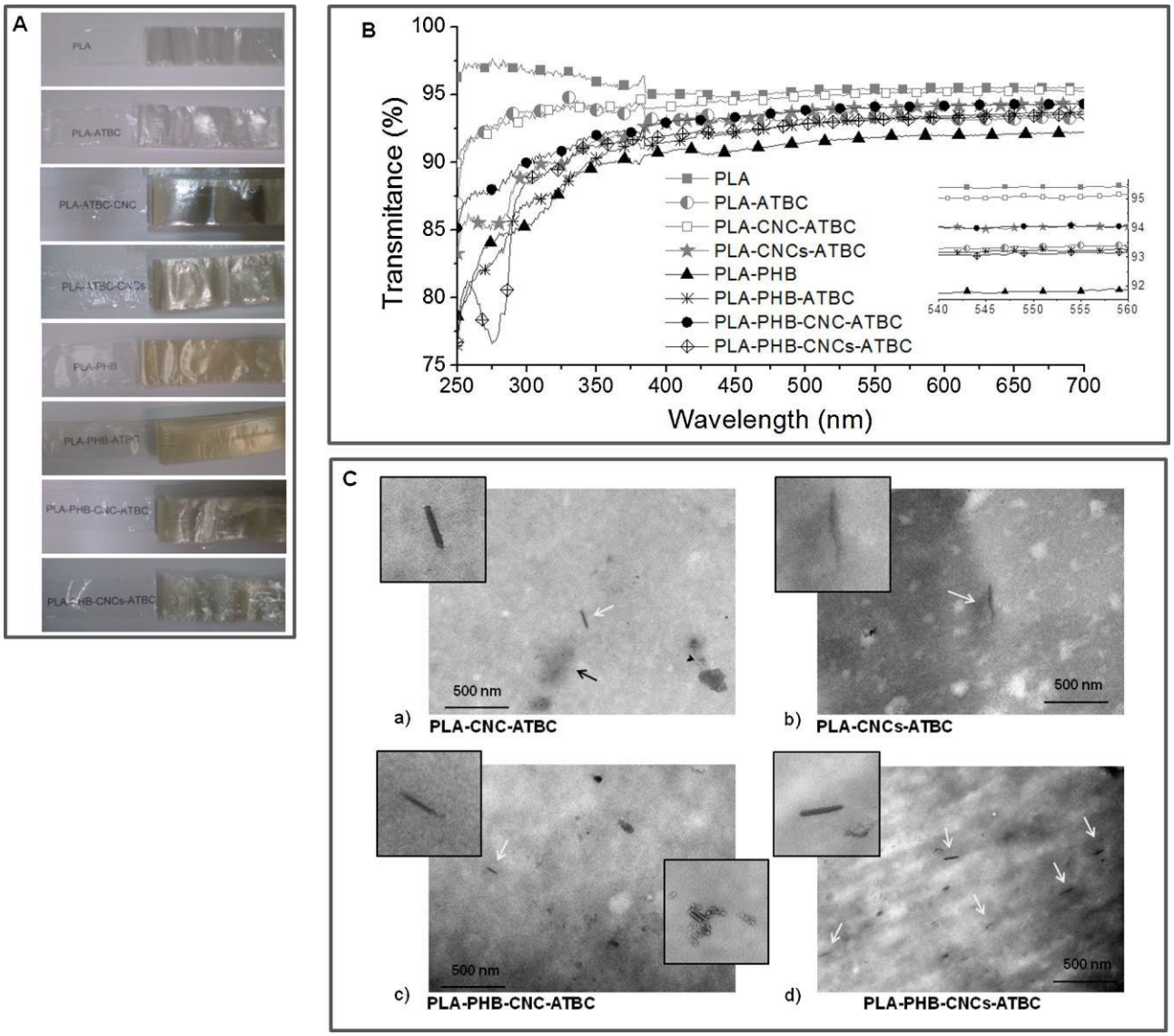

Fig. 1. Plasticized PLA, PLA–PHB and nanocomposite films: (A) visual appearance, (B) UV–vis spectra and (C) TEM analysis of nanocomposite films with cellulose nanocrystals.

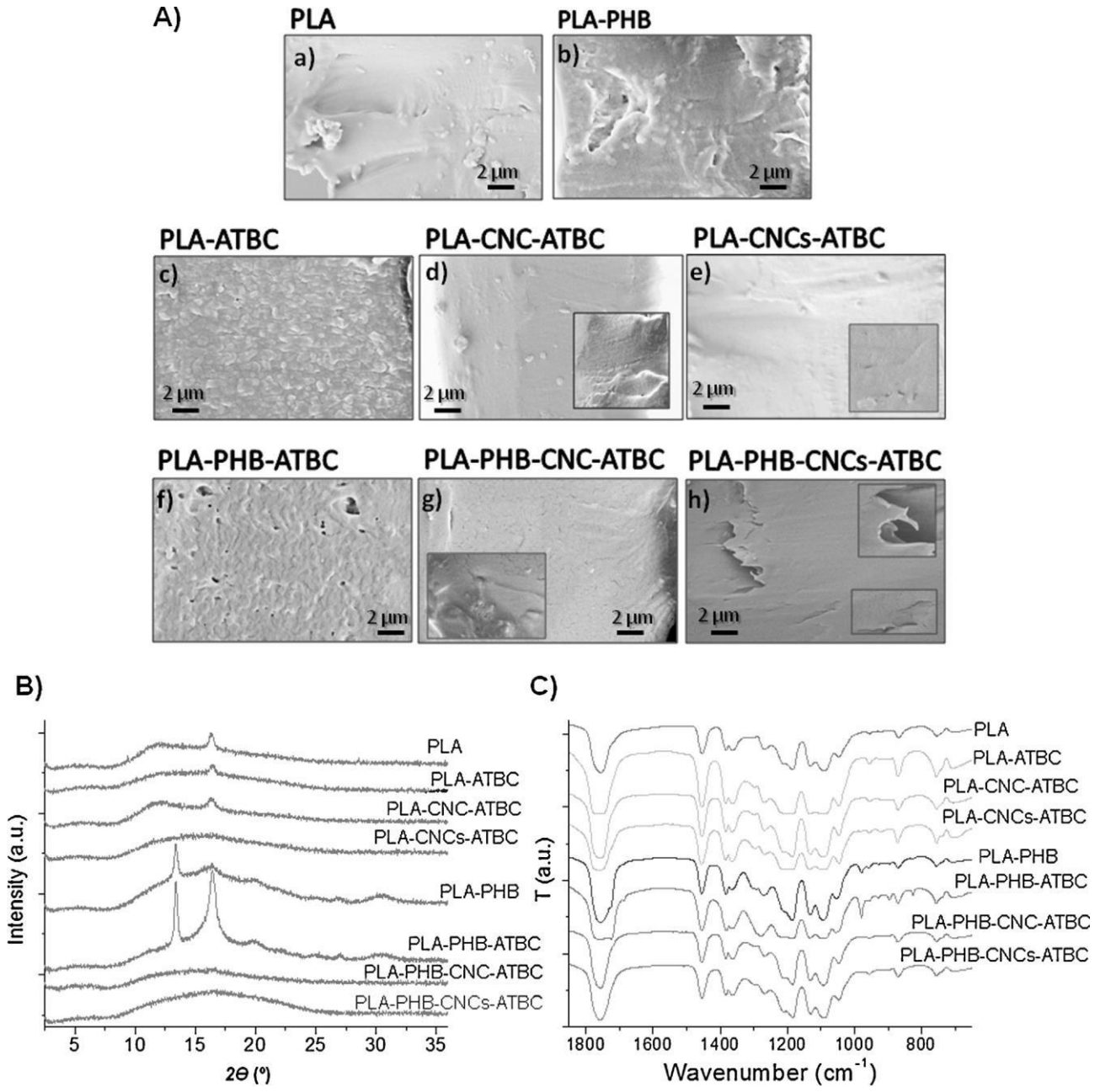

Fig. 2. Plasticized PLA, PLA–PHB and nanocomposite films: (A) microstructure of fracture surface at 20,000× magnifications and inset figure at 35,000× magnifications, (B)X-ray diffraction patterns and (C) FTIR spectra.

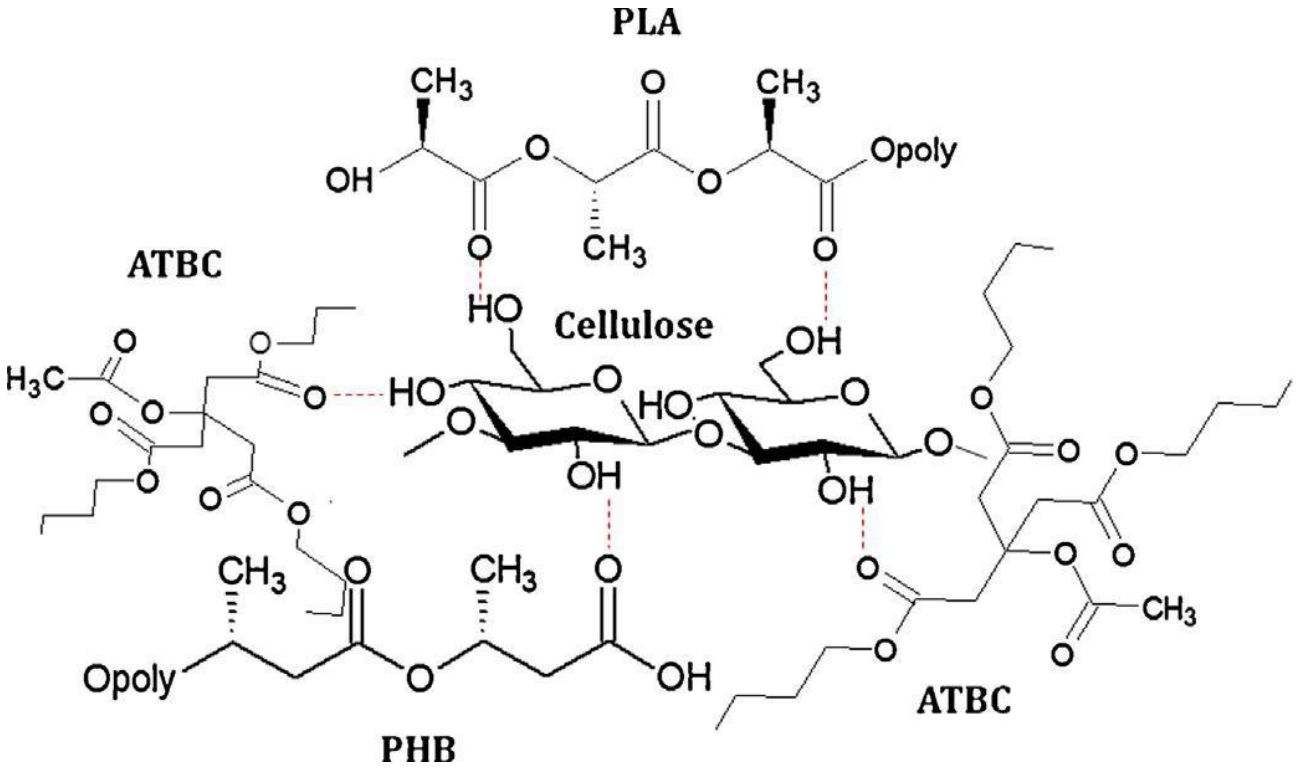

Fig. 3. Proposed molecular interaction between the four components is displayed.

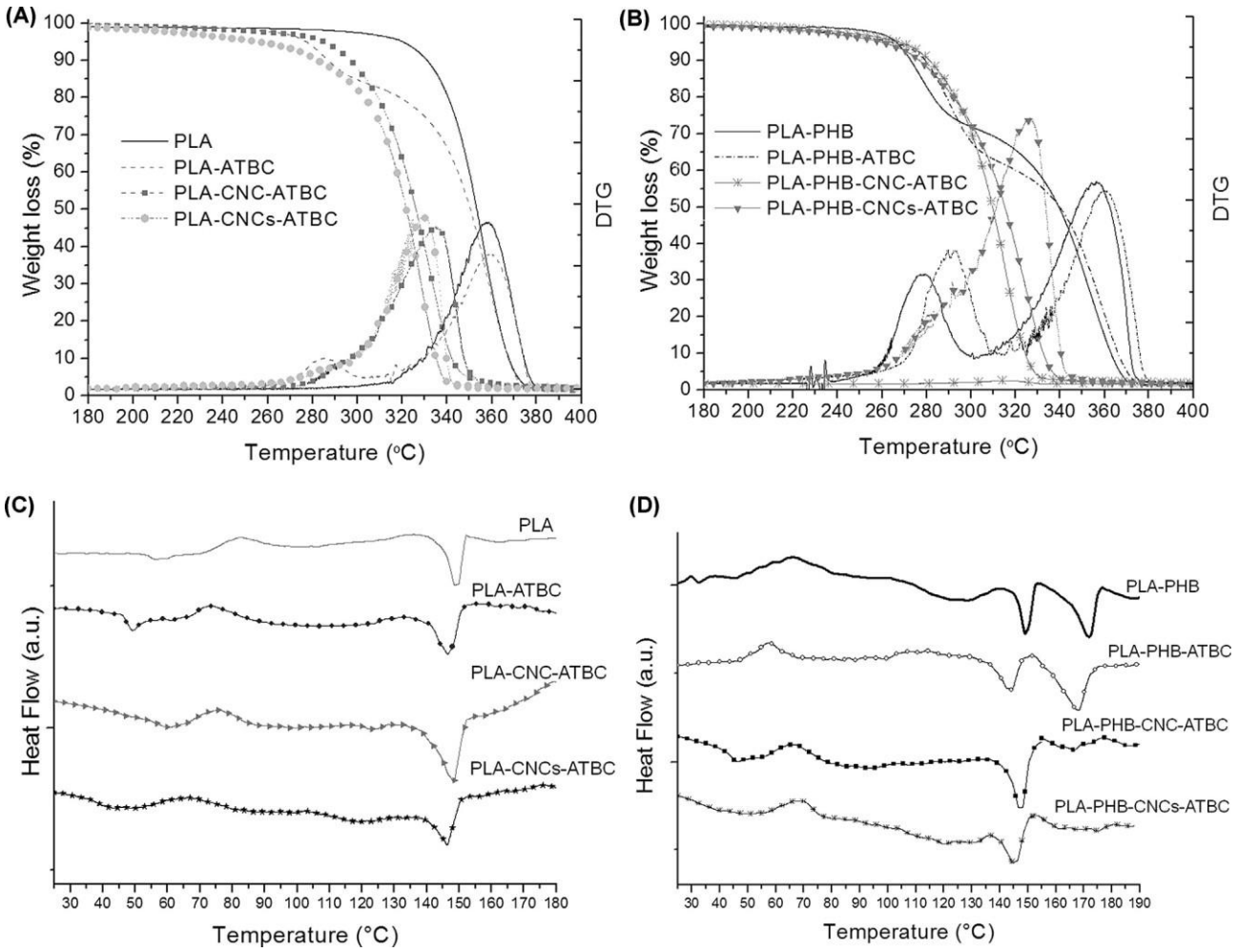

Fig. 4. TG and DTG curves of: (A) plasticized PLA bionanocomposite films and (B) plasticized PLA–PHB bionanocomposite films. DSC curves during first heating scan of: (C)plasticized PLA bionanocomposite films and (D) plasticized PLA–PHB bionanocomposite films.

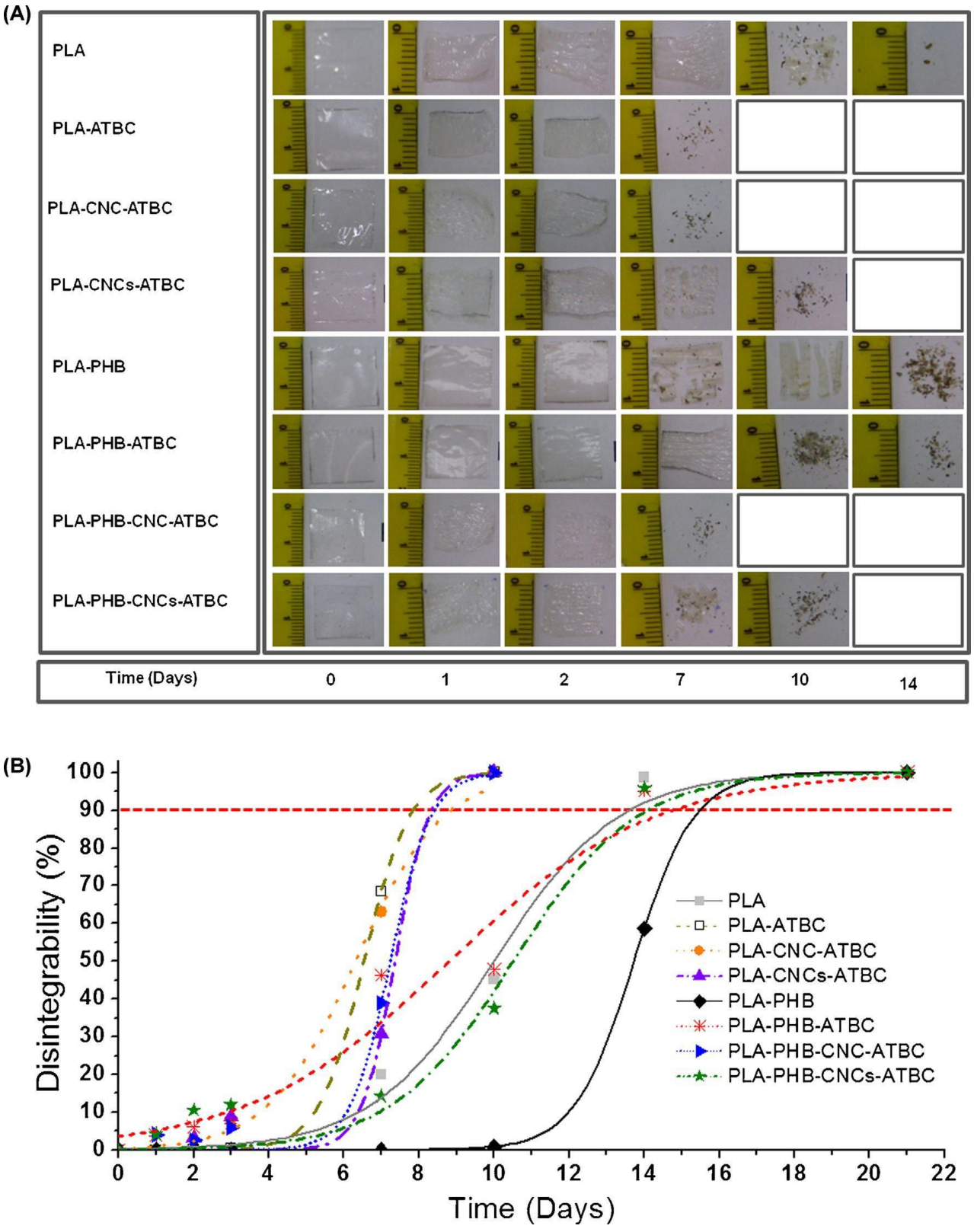

Fig. 5. (A) Visual appearance of film samples before and after different incubation days under composting conditions. (B) Film disintegration degree under composting conditions as a function of time.

Table 1: Bionanocomposite film formulations.

Formulations	PLA (wt%)	PHB (wt%)	CNC (wt%)	CNCs (wt%)	ATBC (wt%)
PLA	100	–	–	–	–
PLA–ATBC	85	–	–	–	15
PLA–CNC–ATBC	80	–	5	–	15
PLA–CNCs–ATBC	80	–	–	5	15
PLA–PHB	75	25	–	–	–
PLA–PHB–ATBC	63.75	21.25	–	–	15
PLA–PHB–CNC–ATBC	60	20	5	–	15
PLA–PHB–CNCs–ATBC	60	20	–	5	15

Table 2: TGA and DSC thermal properties of plasticized PLA and PLA–PHB bionanocomposite films.

Formulations	TGA parameters			DSC parameters (first heating scan)					
	T_0 (°C)	$T_{max\,I}$ (°C)	$T_{max\,II}$ (°C)	T_g (°C)	T_{cc} (°C)	ΔH_{cc} (J g^{-1})	T_m (°C)	ΔH_m (J g^{-1})	χ_c [a] (%)
PLA	320		357	58.8	82.5	12.6	149.0	17.7	5.6
PLA–ATBC	277	285	359	47.3	73.9	24.4	146.7	26.1	2.5
PLA–CNC–ATBC	285	290	335	46.5	75.9	13.4	148.3	33.0	26.2
PLA–CNCs–ATBC	255	282	330	38.9	66.7	20.2	146.4	24.1	28.2
PLA–PHB	266	278	356	53.5	66.4	19.4	149.6/172.7	28.8	11.9
PLA–PHB–ATBC	264	290	360	31.5	75.5	26.7	143.5/167.9	37.3	17.8
PLA–PHB–CNC–ATBC	269	–	317	44.6	67.2	17.5	147.9	31.2	24.3
PLA–PHB–CNCs–ATBC	260	291	326	46.1	95.8	20.2	145.4	40.8	37.0

T_0, calculated at 5% mass loss (10 °C min^{-1}).
DSC parameters calculated at the first heating scan (2 °C min^{-1}).
[a] χ_c (%), calculated using ΔH_m^c of PLA.

Table 3: Tensile test results, water contact angle and time at which 50% of PLA and PLA–PHB bionanocomposite film were degraded in composting conditions

Film formulations	Mechanical properties					Wettability	Disintegration properties
	E (MPa)	σ_Y (MPa)	ε_Y (%)	σ_B (MPa)	ε_B (%)	θ^o	t_{50}
PLA	1240 ± 80^a	52.2 ± 7.8^a	3.5 ± 0.6^{a,b}	46.9 ± 5.4^a	41.1 ± 8.0^{a,d}	83.0 ± 4.2^a	9.99
PLA–ATBC	1110 ± 70^{a,b}	40.9 ± 2.4^b	3.4 ± 0.7^{a,b}	38.3 ± 5.5^a	50.7 ± 0.3^a	75.9 ± 1.9^b	6.54
PLA–CNC–ATBC	1030 ± 50^b	28.1 ± 3.6^{b,c}	2.5 ± 0.5^b	25.8 ± 2.8^b	14.8 ± 0.8^b	69.2 ± 1.2^c	6.31
PLA–CNCs–ATBC	590 ± 60^c	25.7 ± 3.3^c	3.1 ± 0.9^{a,b}	25.0 ± 2.6^b	48.2 ± 2.9^a	78.1 ± 2.1^{a,b}	7.36
PLA–PHB	1810 ± 120^d	44.5 ± 6.7^a	2.9 ± 0.7^a	38.2 ± 18.6^a	13.0 ± 2.1^b	89.8 ± 1.8^d	13.72
PLA–PHB–ATBC	550 ± 30^d	13.3 ± 1.2^d	1.6 ± 0.2^c	40.2 ± 7.0^a	90.1 ± 9.9^c	78.6 ± 2.5^{a,b}	8.82
PLA–PHB–CNC–ATBC	570 ± 90^b	23.7 ± 6.2^{c,d}	3.6 ± 0.9^a	27.3 ± 2.9^b	27.4 ± 3.4^{b,d}	70.7 ± 1.4^{b,c}	7.24
PLA–PHB–CNCs–ATBC	490 ± 20^c	18.9 ± 4.5^{c,d}	4.0 ± 0.6^a	28.2 ± 8.4^b	147.7 ± 15.7^e	68.0 ± 3.1^c	10.51

Different superscripts (a–e) within the same column indicate significant differences between formulations ($p < 0.05$).